

Kink excitation spectra in the (1+1)-dimensional φ^8 model

Vakhid A. Gani,^{1,2,*} Vadim Lensky,^{2,1,†} and Mariya A. Lizunova^{1,2,‡}

¹*National Research Nuclear University MEPhI (Moscow Engineering Physics Institute), 115409 Moscow, Russia*

²*National Research Center Kurchatov Institute, Institute for Theoretical and Experimental Physics, 117218 Moscow, Russia*

Abstract

We study excitation spectra of BPS-saturated topological solutions — the kinks — of the φ^8 scalar field model in $(1 + 1)$ dimensions, for three different choices of the model parameters. We demonstrate that some of these kinks have a vibrational mode, apart from the trivial zero (translational) excitation. One of the considered kinks is shown to have three vibrational modes. We perform a numerical calculation of the kink-kink scattering in one of the considered variants of the φ^8 model, and find the critical collision velocity v_{cr} that separates the different collision regimes: inelastic bounce of the kinks at $v_{\text{in}} \geq v_{\text{cr}}$, and capture at $v_{\text{in}} < v_{\text{cr}}$. We also observe escape windows at some values of $v_{\text{in}} < v_{\text{cr}}$ where the kinks escape to infinity after bouncing off each other two or more times. We analyse the features of these windows and discuss their relation to the resonant energy exchange between the translational and the vibrational excitations of the colliding kinks.

PACS numbers: 11.10.Lm, 11.27.+d, 05.45.Yv, 03.50.-z

*Electronic address: vagani@mephi.ru

†Electronic address: lensky@itep.ru

‡Electronic address: mary.lizunova@gmail.com

I. INTRODUCTION AND MOTIVATION

Topological defects in $(1 + 1)$ space-time dimensions have been a subject of active research [1–3]. Properties of these defects, their interaction with other defects and impurities are widely used to model various phenomena in condensed matter physics [4]. For instance, field models considering a real scalar field with polynomial self-interaction are routinely employed to model phase transitions. The most widely known example of such a model is probably the φ^4 field theory. It has a topological solution — the kink — that can be used to describe a system undergoing a second order phase transition. More complex processes, when a series of consecutive phase transitions is to be modelled, make necessary the use of polynomial self-interactions with the degree higher than four.

Field models that can develop topological solutions are also very important in the context of classical and quantum field theory, high-energy physics, cosmology, as well as hadron and nuclear physics [5–9]. In this relation, one has also to mention the progress in the research of properties of strings, vortices and monopoles [1, 10–22].

To stress the importance of studying topological defects in $(1 + 1)$ dimensions, we note that, while being sufficiently easily treatable, they can correctly describe structures in higher dimensions, such as, for instance, a smooth domain wall in $(3 + 1)$ dimensions whose profile can be described by a $(1 + 1)$ -dimensional kink.

The existence of eigenmodes in the excitation spectrum of a solitary wave is related to its stability against small perturbations; these modes can also affect the interaction of the solitary waves with one another and with external objects. A soliton in a translationally invariant model can always be shifted by a constant vector, which means that there always exists the zero (translational) mode. Excitations with higher energies — vibrational modes — can give rise to a rich collection of resonance phenomena in kink-(anti)kink collisions, as well as in the scattering of kinks off impurities [23–31].

This article deals with topological solitons of the $(1 + 1)$ -dimensional φ^8 field theory. This model has been employed, in particular, to model massless mesons with self-interaction [32], and to describe isostructural phase transitions [33]. We study for the first time the excitation spectra of the kinks that occur in this model, for three different choices of the model’s self-interaction. We show that some of the studied kinks have a vibrational excitation mode. To illustrate how the excitation spectrum of a single kink affects the latter’s interaction with

other kinks (and other spatial defects), we select one of the kinks that have a vibrational excitation and study its collisions with the corresponding antikink.

Our study is structured as follows. Section II provides a brief introduction into general properties of static solutions with finite energy in $(1 + 1)$ dimensions. In Section III, we deal with the kinks of the φ^8 model (with three different choices of the model parameters) and perform a study of their excitation spectra. Section IV presents the results of our numerical study of collisions between one of the kinks that are considered in Section III and the corresponding antikink, and a discussion of the observed resonance phenomena. Section V delivers an outlook and the conclusion.

II. KINKS IN $(1 + 1)$ DIMENSIONS

We consider a field-theory system with a single real scalar field $\varphi(t, x)$ in one spatial and one temporal dimensions, with the Lagrangian

$$\mathcal{L} = \frac{1}{2} (\partial_\mu \varphi)^2 - V(\varphi), \quad \mu = 0, 1, \quad (1)$$

where the self-interaction of the field φ , $V(\varphi)$, is assumed to be bounded from below and hence can be thought of as a non-negative function of φ . The energy functional, corresponding to Eq. (1), is

$$E[\varphi] = \int_{-\infty}^{\infty} \left[\frac{1}{2} \left(\frac{\partial \varphi}{\partial t} \right)^2 + \frac{1}{2} \left(\frac{\partial \varphi}{\partial x} \right)^2 + V(\varphi) \right] dx. \quad (2)$$

The Lagrangian (1) yields the following equation of motion for the field $\varphi(t, x)$:

$$\square \varphi + \frac{dV}{d\varphi} = 0, \quad (3)$$

where $\square = \partial_t^2 - \partial_x^2$ is the d'Alembertian. For a static configuration, $\varphi = \varphi(x)$, this becomes

$$\frac{d^2 \varphi}{dx^2} = \frac{dV}{d\varphi}, \quad (4)$$

which can be transformed into

$$\frac{d\varphi}{dx} = \pm \sqrt{2V(\varphi)} \quad (5)$$

or further into

$$\frac{d\varphi}{dx} = \pm \frac{dW}{d\varphi}, \quad (6)$$

where the superpotential $W(\varphi)$ is related with $V(\varphi)$ via

$$V(\varphi) = \frac{1}{2} \left(\frac{dW}{d\varphi} \right)^2. \quad (7)$$

If the potential $V(\varphi)$ has two or more minima $\bar{\varphi}_1, \bar{\varphi}_2, \dots$, yielding the same minimal value $V(\bar{\varphi}_i) = 0$, $i = 1, 2, \dots$, the energy of a static solution $\varphi = \varphi(x)$ can be written as

$$E = E_{\text{BPS}} + \frac{1}{2} \int_{-\infty}^{\infty} \left(\frac{d\varphi}{dx} \mp \frac{dW}{d\varphi} \right)^2 dx, \quad (8)$$

where

$$E_{\text{BPS}} = |W[\varphi(+\infty)] - W[\varphi(-\infty)]| \quad (9)$$

is the energy of the BPS-saturated solution [2, 34], where the static field $\varphi(x)$ fulfils Eq. (6) and therefore the integrand in Eq. (8) turns into zero. The BPS-saturated solution therefore has the smallest energy among all the static solutions interpolating between two given adjacent minima of the potential,

$$\varphi(-\infty) = \lim_{x \rightarrow -\infty} \varphi(x), \quad \varphi(+\infty) = \lim_{x \rightarrow +\infty} \varphi(x).$$

Note that the static solution $\varphi(x)$ has to converge sufficiently fast to one of the minima of the potential in order that the energy be finite,

$$\lim_{x \rightarrow -\infty} \varphi(x) = \bar{\varphi}_i, \quad \lim_{x \rightarrow +\infty} \varphi(x) = \bar{\varphi}_j \quad (10)$$

(this is also true if the field depends on time). As usual, solutions where $\bar{\varphi}_i = \bar{\varphi}_j$ are called non-topological, whereas $\bar{\varphi}_i \neq \bar{\varphi}_j$ corresponds to a topological solution. We will call the family of all solutions with identical spatial asymptotics a “topological sector”, with the corresponding notation, e.g., $(\bar{\varphi}_i, \bar{\varphi}_j)$ for the topological sector with the asymptotics of Eq. (10).

The field theory being Lorentz-invariant, a static solution of Eq. (4) or Eq. (6) can be boosted to produce a soliton moving with a constant velocity v , with the energy given by

$$E = \frac{M}{\sqrt{1 - v^2}},$$

with M being the energy of the static kink. We reserve the term “kink” (“antikink”) for topological BPS-saturated solutions that connect any two adjacent minima of the self-interaction potential, and their boosts.

In order to analyse the excitation spectrum of a static kink $\varphi_k(x)$, we add to it a small perturbation,

$$\varphi(t, x) = \varphi_k(x) + \delta\varphi(t, x), \quad \|\delta\varphi\| \ll \|\varphi_k\|, \quad (11)$$

and, taking in the equation of motion (3) terms linear in $\delta\varphi(t, x)$, obtain:

$$\frac{\partial^2 \delta\varphi}{\partial t^2} - \frac{\partial^2 \delta\varphi}{\partial x^2} + \left. \frac{d^2 V}{d\varphi^2} \right|_{\varphi_k(x)} \cdot \delta\varphi = 0. \quad (12)$$

Looking for $\delta\varphi(t, x)$ in the form

$$\delta\varphi(t, x) = \psi(x) \cos(\omega t),$$

we obtain from (12) a boundary value problem

$$\left[-\frac{d^2}{dx^2} + \left. \frac{d^2 V}{d\varphi^2} \right|_{\varphi_k(x)} \right] \psi(x) = \omega^2 \psi(x), \quad (13)$$

where $\psi(x)$ has to satisfy the usual Schrödinger-like conditions, i.e., it has to be smoothly differentiable and square integrable over the real axis. The similarity to the Schrödinger equation can be further exploited by denoting

$$U(x) = \left. \frac{d^2 V}{d\varphi^2} \right|_{\varphi_k(x)},$$

making Eq. (13) an eigenvalue problem for the Hamiltonian

$$\hat{H} = -\frac{d^2}{dx^2} + U(x). \quad (14)$$

It can easily be shown that the Hamiltonian (14) always has a zero eigenvalue, corresponding to the translational excitation mode. To demonstrate this, take the derivative of Eq. (4) with respect to x , which gives

$$-\frac{d^2 \varphi'}{dx^2} + \frac{d^2 V}{d\varphi^2} \cdot \varphi' = 0. \quad (15)$$

If we substitute $\varphi = \varphi_k(x)$, this equation becomes an identity (as the kink is a solution of the equation of motion), at the same time coinciding with Eq. (13) if one selects $\omega = 0$. Hence,

$$\psi_0(x) = \varphi'_k(x) \quad (16)$$

is the eigenfunction of the Hamiltonian (14), corresponding to the eigenvalue $\omega = 0$. The square integrability of $\psi_0(x)$ follows from the fact that the energy of the kink is finite, cf. Eq. (2), therefore the eigenvalue $\omega = 0$ belongs to the discrete part of the excitation spectrum.

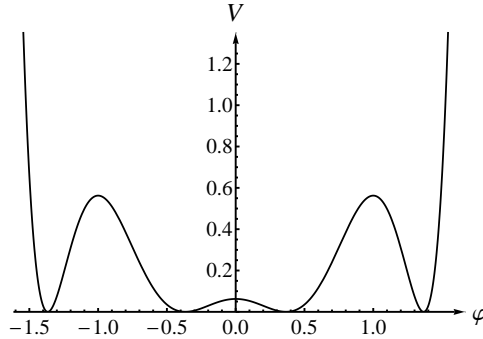


FIG. 1: Plot of the potential with four degenerate minima (17).

III. THE KINKS OF THE φ^8 MODEL AND THEIR EXCITATION SPECTRA

The φ^8 model is described by the Lagrangian (1), where the potential is a polynomial having the degree eight. The shape of the potential can vary depending on the values of the polynomial coefficients. In turn, different shapes of the potential can generate different sequences of phase transitions in condensed matter systems, as shown in ref. [35]. Our choice of the self-interaction parameters follows this reference; the specific potentials that we use have two, three or four degenerate minima, and all are non-negative functions of the field φ .

A. Four degenerate minima

The shape of the potential can in this case be parameterised as

$$V(\varphi) = \lambda^2(\varphi^2 - a^2)^2(\varphi^2 - b^2)^2, \quad (17)$$

where the constants are $0 < a < b$, $\lambda > 0$. The potential (17) has four degenerate minima $\bar{\varphi}_1 = -b$, $\bar{\varphi}_2 = -a$, $\bar{\varphi}_3 = a$, and $\bar{\varphi}_4 = b$. Following ref. [35], we use

$$a = \frac{-1 + \sqrt{3}}{2}, \quad b = \frac{1 + \sqrt{3}}{2}. \quad (18)$$

We also set $\lambda = 1$ in the numerical calculations, which amounts to measuring the potential $V(\varphi)$ in units of λ^2 , while x and t — in units of λ^{-1} . Fig. 1 shows the potential (17) corresponding to the above choice of parameters. For this potential, Eq. (5) gives:

$$\sqrt{2}\lambda x = \int \frac{d\varphi}{\sqrt{(\varphi^2 - a^2)^2(\varphi^2 - b^2)^2}}. \quad (19)$$

Looking at Fig. 1, one can deduce that the kinks that connect the neighbouring vacua belong to either of the three topological sectors $(-b, -a)$, $(-a, a)$, or (a, b) . For example, a static BPS-saturated solution of Eq. (19) interpolating between the vacua $\varphi = -a$ at $x \rightarrow -\infty$ and $\varphi = a$ at $x \rightarrow +\infty$ belongs to the sector $(-a, a)$. At the same time, there is also the corresponding antikink that connects the same vacua, but $\varphi = a$ at $x \rightarrow -\infty$ and $\varphi = -a$ at $x \rightarrow +\infty$. Formally, it belongs to the topological sector $(a, -a)$; the distinction between kinks and antikinks is, however, just a matter of convention, and we will not distinguish between the sectors $(-a, a)$ and $(a, -a)$ and will drop the prefix “anti”, unless the opposite is needed in order to avoid confusion or to explicitly identify the field configuration in question.

The kinks corresponding to the three topological sectors above can be obtained from Eq. (19) as implicit functions of x [32, 35]. Below, we examine their excitation spectra.

1. Topological sector $(-a, a)$

This kink is constrained by $|\varphi| < a$, which allows Eq. (19) to be rewritten as

$$\sqrt{2}\lambda x = \int \frac{d\varphi}{(a^2 - \varphi^2)(b^2 - \varphi^2)}.$$

The corresponding implicit solution is [32, 35]:

$$e^{\mu x} = \frac{a + \varphi}{a - \varphi} \left(\frac{b - \varphi}{b + \varphi} \right)^{a/b}, \quad (20)$$

where $\mu = 2\sqrt{2}\lambda a(b^2 - a^2)$. This equation can be solved for $\varphi(x)$ numerically, and the plot of this kink is shown in Fig. 2 (left panel). The corresponding antikink can be obtained from Eq. (20) by substituting $x \rightarrow -x$:

$$e^{-\mu x} = \frac{a + \varphi}{a - \varphi} \left(\frac{b - \varphi}{b + \varphi} \right)^{a/b}. \quad (21)$$

Using Eq. (2) or Eq. (9) gives the energy (mass) of the static kink:

$$M_{(-a,a)} = \frac{4\sqrt{2}}{15} \lambda a^3 (5b^2 - a^2).$$

We performed a numerical search of excitations of the kink (20) lying in the discrete part of the excitation spectrum. Fig. 2 (right panel) shows the corresponding potential $U(x)$ that enters the Schrödinger eigenvalue problem. This problem was solved using the standard

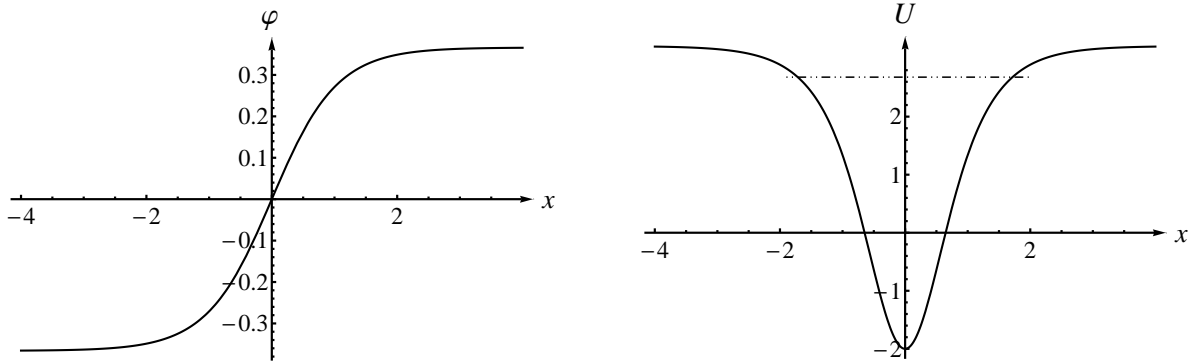


FIG. 2: **Left panel** — the solution of Eq. (20) that connects the vacua $-a$ and a . **Right panel** — the potential $U(x)$ corresponding to the kink shown in the left panel. The dashed line shows the value of ω_1^2 .

methods, namely, integrating Eq. (13), with the known asymptotic behaviour of its solutions at $x \rightarrow \pm\infty$, starting at a large negative $x = x_l$ (the “left” solution) and a large positive $x = x_r$ (the “right” solution). The two solutions were then matched at some point \tilde{x} close to the spatial origin. The specific choice of \tilde{x} is not very important, for instance, one could take $\tilde{x} = 0$, however, it is convenient to take a small offset from the zero value — this helps to avoid technical issues when $U(x)$ is an even function of x (in this case, excitation profiles $\psi(x)$ are either even or odd functions of x , and the latter ones have a node at $x = 0$). We selected those values of ω at which the Wronskian of the “left” and the “right” solution, calculated at the matching point, turns to zero.

We found two eigenvalues, $\omega_0^2 = -2 \times 10^{-8}$, and $\omega_1^2 = 2.70491$. The former value is just the translational mode, whose exact energy is $\omega_0 = 0$; the deviation of our numerical result from zero thus provides an estimate of accuracy. The latter value corresponds to the vibrational excitation, whose existence is non-trivial and reflects itself in resonance phenomena occurring in kink-antikink collisions in this topological sector, see Sec. IV.

2. Topological sector $(-b, -a)$

In this sector $a < |\varphi| < b$, which turns (19) into

$$\sqrt{2}\lambda x = \int \frac{d\varphi}{(\varphi^2 - a^2)(b^2 - \varphi^2)}.$$

Taking the integral results in

$$e^{\mu x} = \frac{\varphi - a}{\varphi + a} \left(\frac{b + \varphi}{b - \varphi} \right)^{a/b}, \quad (22)$$

where $\mu = 2\sqrt{2}\lambda a(b^2 - a^2)$; note that the kink that connects the vacua a and b can be directly obtained from this expression. The static kink (22) has the mass

$$M_{(-b,-a)} = \frac{2\sqrt{2}}{15}\lambda(b-a)^3(a^2 + 3ab + b^2);$$

its profile is shown in Fig. 3 (left panel).

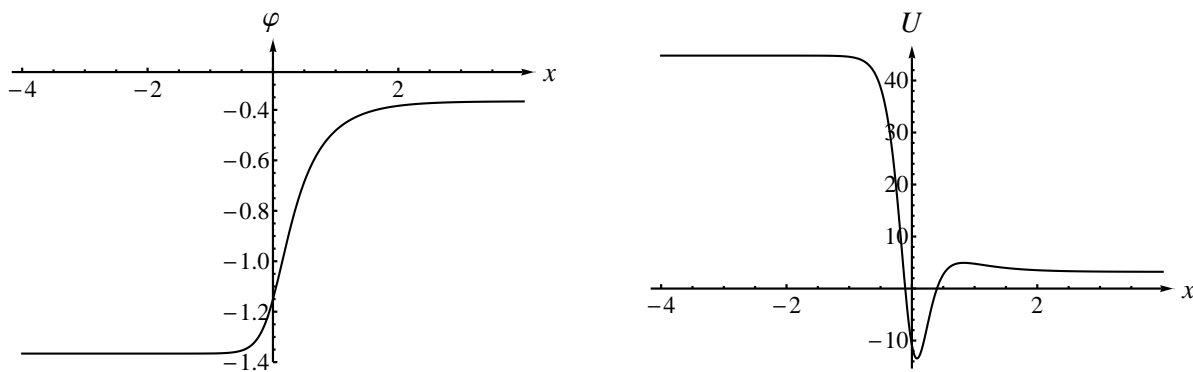


FIG. 3: **Left panel** — the kink (22) that connects the vacua $-b$ and $-a$. **Right panel** — the potential $U(x)$ corresponding to the kink shown in the left panel.

As opposed to the sector $(-a, a)$, we found the kink (22) of the sector $(-b, -a)$ (which applies to that of the sector (b, a) , too) to only have the trivial translational excitation, the numerical value being $\omega_0^2 = -7 \times 10^{-8}$. The corresponding potential entering the Schrödinger equation is shown in the right panel of Fig. 3. It has to be noted that, even though the kinks considered in this subsection do not have a vibrational excitation, a static kink and the corresponding static antikink located close to each other can still have a vibrational mode. Notice that even though such a configuration is not a solution of the equation of motion, due to the nonlinear character of the field interaction, the introduced error typically falls off exponentially with increasing separation between the two solitons, which is why such Ansätze are routinely employed. The existence of such a “collective” vibrational mode can manifest itself as resonance phenomena in kink-antikink collisions. Realisations of this mechanism have been studied, for instance, in refs. [36, 37].

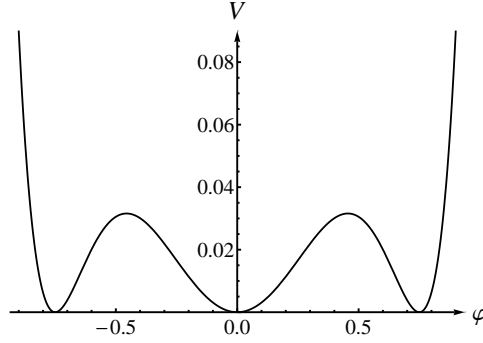


FIG. 4: Plot of the potential with three degenerate minima (23).

B. Three degenerate minima

This situation corresponds to the potential taking the form

$$V(\varphi) = \lambda^2 \varphi^2 (\varphi^2 - a^2)^2 (\varphi^2 + b^2), \quad (23)$$

where the constants satisfy $a > 0$, $b > 0$, $\lambda > 0$. This potential has three degenerate minima: $\bar{\varphi}_1 = -a$, $\bar{\varphi}_2 = 0$, and $\bar{\varphi}_3 = a$. The corresponding topological sectors are $(-a, 0)$ and $(0, a)$. Following ref. [35], our choice of parameters is

$$a = \frac{3}{4}, \quad b = 1.$$

Fig. 4 shows the plot of the resulting potential. Obviously, the sectors $(-a, 0)$ and $(0, a)$ are related by a change of the sign of $\varphi(t, x)$, hence only one of the two sectors has to be studied. Eq. (5) with the potential (23) results in the following implicit expression for the kink that connects $\bar{\varphi}_2 = 0$ and $\bar{\varphi}_3 = a$:

$$e^{\mu x} = \left(\frac{\sqrt{b^2 + a^2} + \sqrt{b^2 + \varphi^2}}{\sqrt{b^2 + a^2} - \sqrt{b^2 + \varphi^2}} \right) \cdot \left(\frac{\sqrt{b^2 + \varphi^2} - b}{\sqrt{b^2 + \varphi^2} + b} \right)^{\sqrt{b^2 + a^2}/b}, \quad (24)$$

where $\mu = 2\sqrt{2}\lambda a^2 \sqrt{a^2 + b^2}$, with the mass of this kink being

$$M_{(0,a)} = \frac{\sqrt{2}}{15} \lambda (2(b^2 + a^2)^{5/2} - b^3(2b^2 + 5a^2)).$$

Fig. 5 shows a plot of the kink (24) in the left panel and of the corresponding Schrödinger potential in the right panel. Our study of the excitation spectrum of this kink found only the translational mode, with the numerical result for the eigenvalue $\omega_0^2 = 4 \times 10^{-8}$.

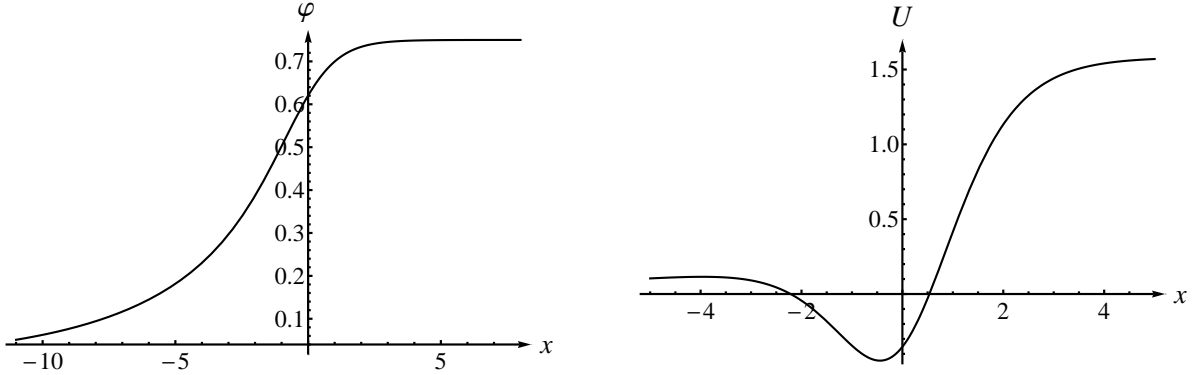


FIG. 5: **Left panel** — the kink (24) that connects the vacua 0 and a . **Right panel** — the potential $U(x)$ corresponding to the kink in the left panel.

C. Two degenerate minima

The self-interaction potential of the φ^8 model can in this case be written as

$$V(\varphi) = \lambda^2(\varphi^2 - a^2)^2(\varphi^2 + b^2)^2, \quad (25)$$

where $a > 0$, $b > 0$, $\lambda > 0$. The two degenerate minima are $\bar{\varphi}_1 = -a$ and $\bar{\varphi}_2 = a$, and there is only one kink that connects the points $-a$ and a , and its antikink counterpart. The parameters we use are [35]:

$$a = \frac{4}{5}, \quad b = 1.$$

The potential (25) with these parameters is plotted in Fig. 6.

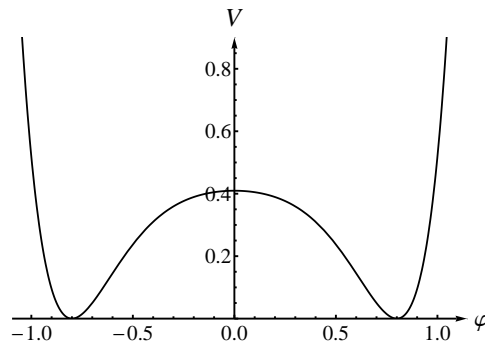


FIG. 6: Plot of the potential with two degenerate minima (25).

The static kink belonging to the topological sector $(-a, a)$ is, as usual, obtained from the equation of motion (5):

$$\mu x = \frac{2a}{b} \tan^{-1} \left(\frac{\varphi}{b} \right) + \log \left(\frac{a + \varphi}{a - \varphi} \right), \quad (26)$$

where $\mu = 2\sqrt{2}\lambda a(b^2 + a^2)$. The mass of this kink is

$$M_{(-a,a)} = \frac{4\sqrt{2}}{15}\lambda a^3(a^2 + 5b^2).$$

Fig. 7 shows the kink (26) in the left panel, and the corresponding quantum-mechanical potential that defines small excitations of this kink in the right panel.

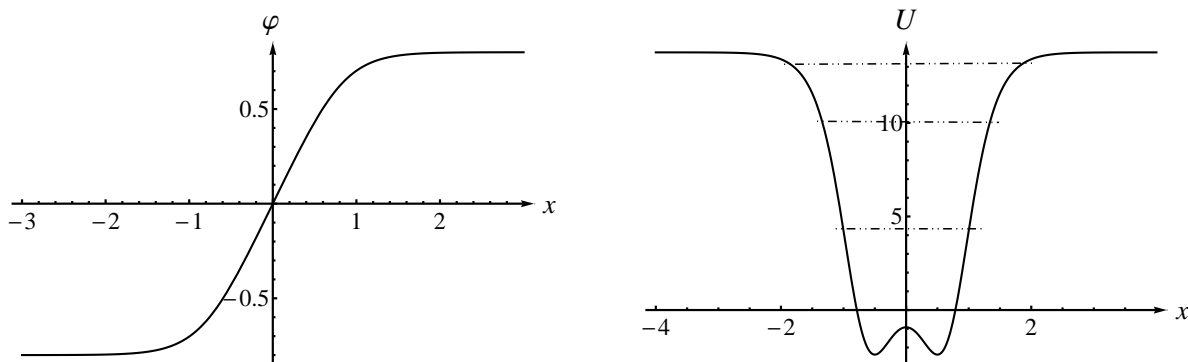


FIG. 7: **Left panel** — the kink (26) that connects the vacua $-a$ and a . **Right panel** — the potential $U(x)$ that corresponds to this kink. The dashed lines show the values of ω_1^2 , ω_2^2 , and ω_3^2 , ordered from bottom to top.

The kink of this specific realisation of the φ^8 model yields the richest set of eigenmodes: besides the translational mode (with the numerical value of $\omega_0^2 = 5 \cdot 10^{-9}$), we found three vibrational excitations with energies $\omega_1^2 = 4.27575$, $\omega_2^2 = 10.1893$, and $\omega_3^2 = 13.6095$.

A few more words are in order regarding the numerical accuracy. As stated above, the deviation of the numerical result for ω_0^2 from zero can serve as an estimate of the numerical error of the energy values. On the other hand, regarding the precision of the excitation profiles $\psi(x)$, one can, for instance, check that the profiles corresponding to different eigenvalues (where there are excitations other than the translational mode) are orthogonal. The results of this check are given in Table I.

IV. KINK-KINK COLLISIONS

The existence of a vibrational excitation of a kink means that, in certain conditions, kinetic energy of the moving kink can be transferred to and stored in the form of small oscillations of the kink's profile. This is known to lead to interesting phenomena in kink-kink collisions [3, 23, 36–40].

TABLE I: Eigenvalues and orthogonality checks (where applicable) of the kinks considered in Sec. III; $\psi_i(x)$ are normalised to unity.

Kink	x_l	x_r	Eigenvalue	Orthogonality check
(20)	-9	9	$\omega_0^2 \simeq -2 \times 10^{-8}$	—
			$\omega_1^2 \simeq 2.70491$	$(\psi_0, \psi_1) \simeq -1 \times 10^{-7}$
(22)	-9	9	$\omega_0^2 \simeq -7 \times 10^{-8}$	—
(24)	-42	13	$\omega_0^2 \simeq 4 \times 10^{-8}$	—
(26)	-10	10	$\omega_0^2 \simeq 5 \times 10^{-9}$	—
			$\omega_1^2 \simeq 4.27575$	$(\psi_0, \psi_1) \simeq 1 \times 10^{-10}$
			$\omega_2^2 \simeq 10.1893$	$(\psi_0, \psi_2) \simeq 4 \times 10^{-8}$ $(\psi_1, \psi_2) \simeq 2 \times 10^{-9}$
			$\omega_3^2 \simeq 13.6095$	$(\psi_0, \psi_3) \simeq -4 \times 10^{-8}$ $(\psi_1, \psi_3) \simeq 2 \times 10^{-5}$ $(\psi_2, \psi_3) \simeq 2 \times 10^{-6}$

As an illustrative example, we performed a numerical calculation of the kink-antikink scattering in one of the topological sectors of the variant of the φ^8 theory with four degenerate minima, i.e., with the field self-interaction given by Eq. (17). We studied a configuration constructed from the kink (20) and the corresponding antikink (21). Namely, we set the initial field profile to

$$\varphi(t, x) = \varphi_{(-a, a)} \left(\frac{x + x_0 - v_{\text{in}} t}{\sqrt{1 - v_{\text{in}}^2}} \right) + \varphi_{(a, -a)} \left(\frac{x - x_0 + v_{\text{in}} t}{\sqrt{1 - v_{\text{in}}^2}} \right) - a, \quad (27)$$

where $\varphi_{(-a, a)}(x)$ and $\varphi_{(a, -a)}(x)$ are the static kink and the static antikink. This setup corresponds to the kink and the antikink, separated at $t = 0$ by $2x_0$, and moving towards each other with the velocities $\pm v_{\text{in}}$ in the laboratory frame. As the separation between the kinks increases, the overlap between them becomes exponentially small and they stop being affected by each other — this happens in the asymptotic regime of the collision. In practice, the initial separation $2x_0$ has to be much larger than the typical width of the kink; in our calculation, we use $2x_0 = 25$.

We solved the equation of motion using the standard explicit finite difference scheme,

$$\varphi_{tt} = \frac{\varphi_j^{k+1} - 2\varphi_j^k + \varphi_j^{k-1}}{\tau^2}, \quad \varphi_{xx} = \frac{\varphi_{j+1}^k - 2\varphi_j^k + \varphi_{j-1}^k}{h^2},$$

where τ and h are, respectively, the time and space grid spacings, and (k, j) number the corresponding coordinates of the grid points, (t_k, x_j) . The initial conditions follow from Eq. (27), and the presented results correspond to $\tau = 0.002$ and $h = 0.01$. The infinite space domain was truncated, so that $-l \leq x \leq l$, with $l = 100$, whereas the time varied in the range $0 \leq t \leq 900$. As dictated by the dependence domains, the calculation started from a much larger interval of the x axis at $t = 0$ (namely, $-4650 \leq x \leq 4650$). To check our numerical results, we tested the conservation of energy as the time evolution progressed, taking into account energy flux through the endpoints of the space interval:

$$\int_{-l}^l \left[\frac{1}{2} \left(\frac{\partial \varphi}{\partial t} \right)^2 + \frac{1}{2} \left(\frac{\partial \varphi}{\partial x} \right)^2 + V(\varphi) \right] dx - \int_0^{t_c} \frac{\partial \varphi}{\partial t} \frac{\partial \varphi}{\partial x} \Big|_{-l}^l dt = \frac{2M}{\sqrt{1 - v_{\text{in}}^2}},$$

where t_c is the current moment of time (the integrand in the first integral is evaluated at $t = t_c$).

Our numerical simulations showed several different scattering regimes can realise, depending on the initial collision speed. We found out that there is a critical speed $v_{\text{cr}} \simeq 0.3160$ such that at $v_{\text{in}} \geq v_{\text{cr}}$ the kinks bounce off each other and escape, as illustrated in Fig. 8. The kink-antikink scattering is only approximately elastic, i.e., the asymptotic escape velocity $v_f < v_{\text{in}}$. This feature can be seen in Fig. 8 as well; the typical values are, e.g., $v_f = 0.23$ at $v_{\text{in}} = 0.40$, $v_f = 0.36$ at $v_{\text{in}} = 0.50$, and $v_f = 0.47$ at $v_{\text{in}} = 0.60$.

As opposed to the previous regime, collision velocities $v_{\text{in}} < v_{\text{cr}}$ result in the formation of a long-lived bound state of the two kinks, the bion, see Fig. 9. This, however, does not hold for all $v_{\text{in}} < v_{\text{cr}}$; there are intervals of the collision velocities — the escape windows — where kinks still escape to the spatial infinity albeit only after having collided two, three, or more times. Similar processes have been observed in other field models, see, e.g., [3] for review. This phenomenon has been explained by resonant energy exchange between the translational mode and a localized excitation mode of the kink. The value of the corresponding resonance frequency ω_R in some models coincides with the kink vibrational mode frequency ω_1 , whereas in other field models ω_R could significantly deviate from ω_1 [37, 38], or even belong to the continuous part of the excitation spectrum [39]. During the first collision, the kinetic energy

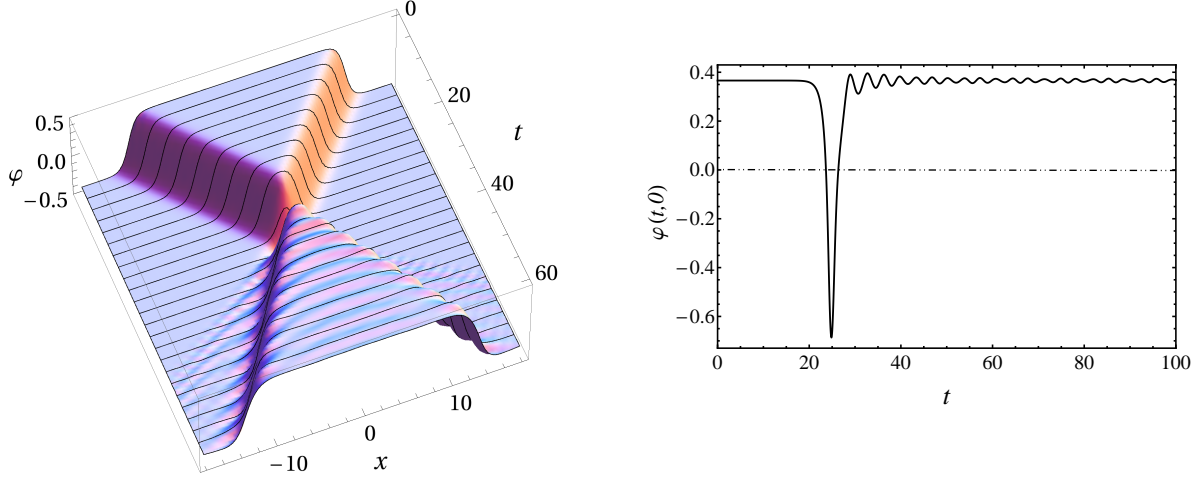


FIG. 8: (Inelastic) kink-kink scattering at $v_{\text{in}} = 0.5000$. **Left panel** — space-time evolution of the system. **Right panel** — $\varphi(t, 0)$, the time profile of the field at $x = 0$.

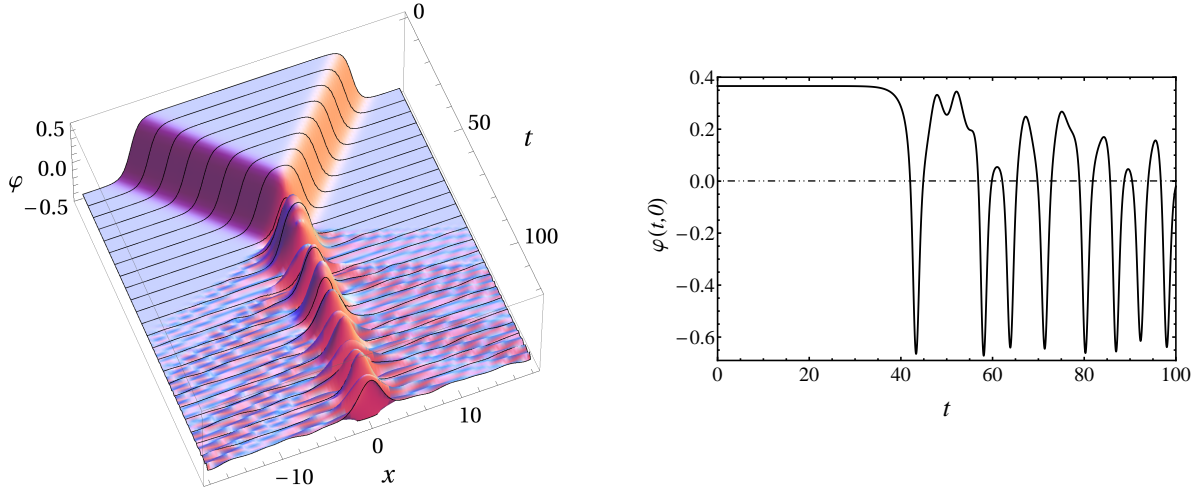


FIG. 9: Bion formation at $v_{\text{in}} = 0.2740$. **Left panel** — space-time evolution. **Right panel** — the profile of $\varphi(t, 0)$.

of the kinks can partly be transferred to the mode ω_R . After that, the kinks bounce but cannot escape, and hence they stop at some point and then collide again. However, the second collision may result in transfer of the energy of the mode ω_R back to the kinetic energy. This can happen if the time T_{12} between the collisions and the frequency ω_R are in a certain resonance relation (see below), and, as a result, the kinks can escape after the second collision. An example of such a two-bounce is shown in Fig. 10. Note that this regime is also inelastic — the kinks lose a part of their initial kinetic energy; this can be seen in the figures as well. We found around twenty two-bounce escape windows, as well as a number of three-

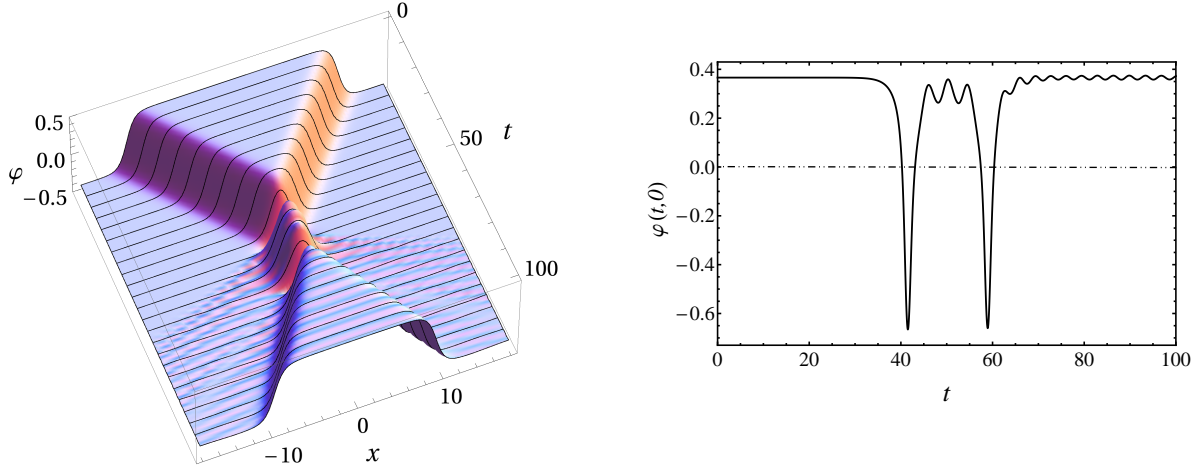


FIG. 10: Two-bounce at $v_{\text{in}} = 0.2868$. **Left panel** — space-time evolution. **Right panel** — the profile of $\varphi(t, 0)$.

and four-bounce escape windows (where the kinks escape to infinity after three and four collisions). Fig. 11 shows the positions of these φ^8 model escape windows and demonstrates

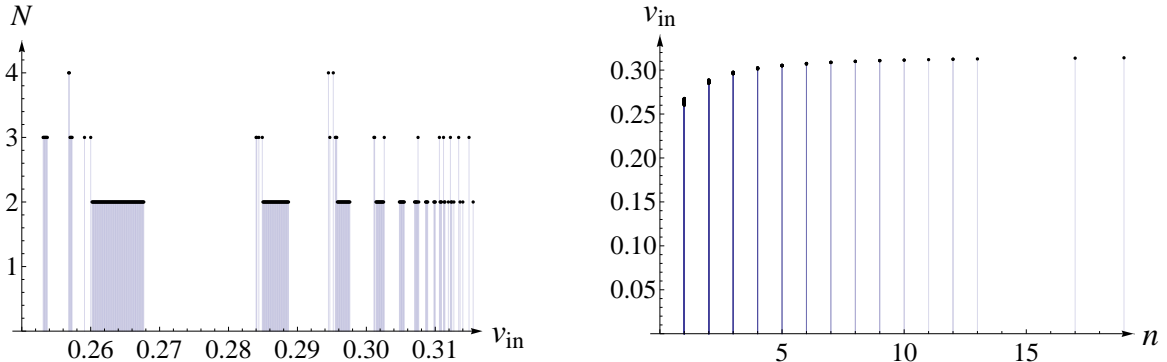


FIG. 11: **Left panel** — Quasi-fractal structure of the escape windows; here N is the number of collisions before escape. **Right panel** — locations of two-bounce escape windows versus n , the number of small oscillations (see text for the definition).

that they exhibit features similar to observed, e.g., in the φ^4 model [3], namely, the quasi-fractal structure and the concentration of resonances near the critical velocity v_{cr} . We also analysed the positions of the two-bounce escape windows, using phenomenological relations that have been applied to resonance kink-kink collisions in other models, cf. ref. [3]. The main results of this analysis are shown in Fig. 12 and in Table II.

The first of the relations in question connect the resonance frequency ω_R with the number n of small oscillations of the field at $x = 0$ between the two collisions (so that, e.g., the two-

bounce shown in Fig. 10 corresponds to $n = 2$):

$$\omega_R T_{12} = 2\pi(n + 2) + \delta = 2\pi\tilde{n} + \delta, \quad (28)$$

where δ is a constant phase shift. Note that n can also be viewed as the number of the respective escape window in the sequence shown in Fig. 11 (implying that the windows with numbers 14, 15, 16, and 18 are missing — we have not observed them in our numerical simulations). The shift of n by two in Eq. (28) is dictated by our choice that δ has to be between 0 and 2π . Fig. 12 shows T_{12} as a function of \tilde{n} . As one can see from this figure, the linear dependence of Eq. (28) fits nicely the numerical results, with the values of the resonance parameters resulting from the fit being $\omega_R = 1.618$ and $\delta = 3.403$. This value of ω_R is slightly less than the frequency of the kink’s vibrational excitation, $\omega_1 = 1.644$. This can be attributed to the interaction between the two kinks: it continuously distorts the excitation spectrum of the kink-kink system during the collision, which (inter alia) can lead to a deviation of ω_R from ω_1 [37]. As mentioned above, the collective excitation spectrum of the kink-kink system can have a vibrational mode even when either of the solitary kinks does not. This feature gives rise to resonance phenomena such as escape windows and quasi-resonances in models such as φ^6 where the kinks only have the translational excitation [36].

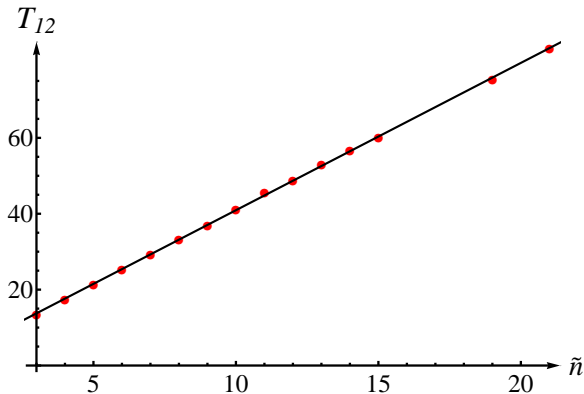


FIG. 12: Time between the first two collisions T_{12} as a function of \tilde{n} for two-bounce escape windows. Dots show results of our numerical calculations, the solid line is the corresponding linear fit of Eq. (28).

Table II collects information we have obtained on two-bounce escape windows. It lists the initial collision velocities v_{in} (taken at the midpoint of the corresponding window), the final

escape velocities v_f , and the values of T_{12} . We also applied the phenomenological analysis of ref. [39], calculating

$$\beta = T_{12} \sqrt{v_{\text{cr}}^2 - v_{\text{in}}^2} \quad (29)$$

for each of the escape windows, with the mean value being $\bar{\beta} \simeq 2.569$. The latter quantity was used to predict the locations of escape windows:

$$v_{\text{in}}^{\text{theor}}(n) = v_{\text{cr}} - \frac{\bar{\beta}^2 \omega_R^2}{2v_{\text{cr}}(2\pi\tilde{n} + \delta)^2}, \quad (30)$$

where $v_{\text{in}}^{\text{theor}}$ is the predicted escape window initial velocity, assuming small deviation of the latter from the critical velocity, $v_{\text{in}} \simeq v_{\text{cr}}$. Table II shows that Eq. (30) does not provide accurate predictions for v_{in} — theoretical values at large values of n can differ from the corresponding calculated values by an amount larger than the distance between two adjacent escape windows. This is at least partly due to poor accuracy of the determination of $\bar{\beta}$, which has a scatter of about 15%. We have thus not been able to use Eq. (30) to pinpoint the location of the escape windows with $n = 14, 15, 16, 18$ that had not been observed directly in the numerical calculations.

As mentioned above, in our calculations we also observed three-bounces and four-bounces — in these cases the kinetic energy is (partly) restored only after three and four collisions, respectively. Typical space-time pictures of these processes are shown in Figs. 13 and 14.

Another resonance feature, observed previously in kink-kink collisions in the double sine-

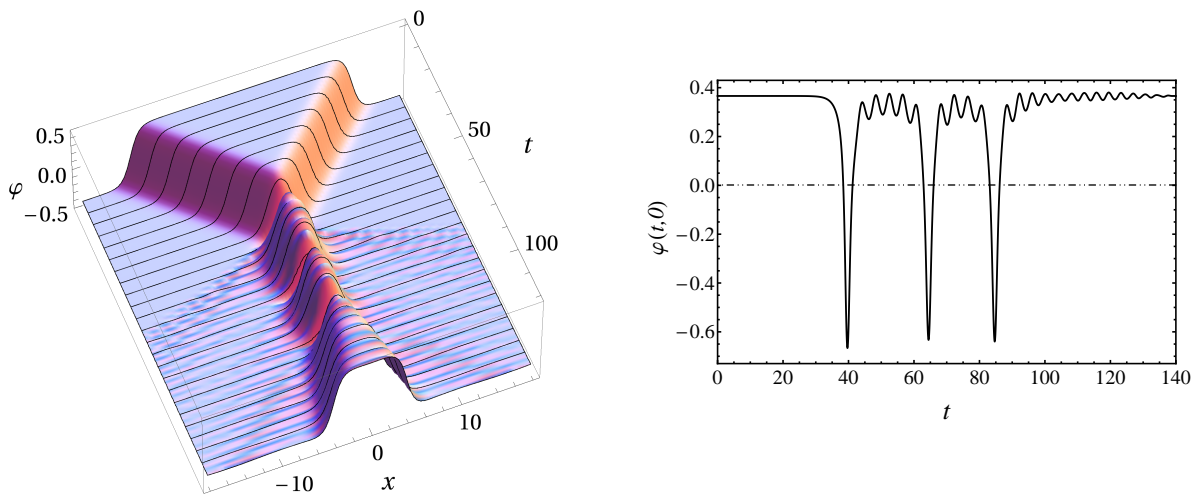


FIG. 13: Three-bounce at $v_{\text{in}} = 0.3012$. **Left panel** — space-time evolution. **Right panel** — the profile of $\varphi(t, 0)$.

TABLE II: Two-bounce escape windows. The values of v_{in} are given at the midpoint of the corresponding escape window.

n	v_{in}	v_{f}	T_{12}	β	$v_{\text{in}}^{\text{theor}}$
1	0.2639	0.158	13.446	2.337	0.2608
2	0.2868	0.207	17.422	2.311	0.2824
3	0.2967	0.229	21.424	2.330	0.2934
4	0.3019	0.239	25.386	2.370	0.2998
5	0.3051	0.237	29.256	2.407	0.3038
6	0.3073	0.247	33.280	2.451	0.3065
7	0.3087	0.214	36.940	2.495	0.3084
8	0.3099	0.253	41.180	2.545	0.3098
9	0.3108	0.079	45.528	2.599	0.3108
10	0.3113	0.222	48.678	2.643	0.3116
11	0.3119	0.253	52.892	2.684	0.3122
12	0.3123	0.249	56.624	2.730	0.3127
13	0.3127	0.124	60.058	2.736	0.3131
17	0.3136	0.041	75.466	2.934	0.3142
19	0.3140	0.221	83.542	2.965	0.3145

Gordon [37, 38] as well as in the modified sine-Gordon model [39], is quasi-resonances. They occur when the energy that is pumped back into the translational mode during the second collision is not enough for the two kinks to escape. The two kinks merely come some large but finite distance apart and then collide again, eventually merging into the bion. This situation shows as a peak on the plot of T_{23} , the time between the second and the third collisions, as a function of the initial velocity v_{in} . In some models, quasi-resonances have been shown to replace some of the escape windows [37], which is not unexpected as both these phenomena are due to the resonant energy exchange. Our calculation has not shown any clear signs of quasi-resonances occurring in the considered variant of the φ^8 model.

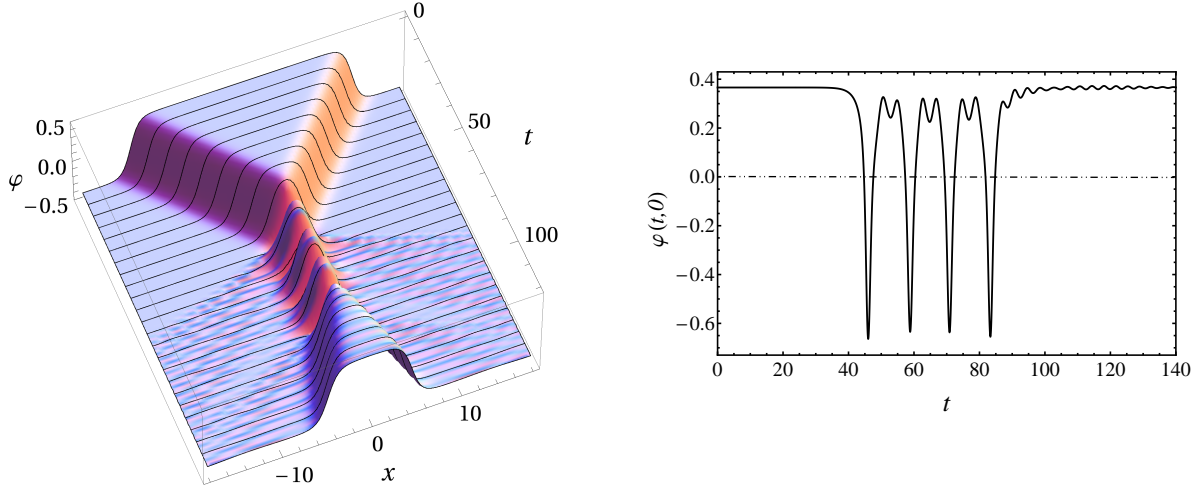


FIG. 14: Four-bounce at $v_{\text{in}} = 0.2568$. **Left panel** — space-time evolution. **Right panel** — the profile of $\varphi(t, 0)$.

V. SUMMARY AND DISCUSSION

We studied excitation spectra of the φ^8 field model, choosing three different sets of the model's self-interaction potential. We found that some of the kinks that arise in those variants of the φ^8 model have vibrational excitation modes, which points at the possibility for resonance phenomena to occur in low-energy kink-kink scattering. To illustrate that relation between the excitation of a solitary kink and the kink-kink scattering, we performed numerical modelling of the latter process, using one of the considered kinks that has a vibrational excitation, and the corresponding antikink. We showed that there are two collision regimes, depending on the initial velocity of the two colliding kinks. Namely, the kinks bounce off each other inelastically at $v_{\text{in}} \geq v_{\text{cr}}$, whereas $v_{\text{in}} < v_{\text{cr}}$ results in the formation of a bound state of two kinks, the bion. Furthermore, we demonstrated the existence of escape windows — intervals of initial velocities in the domain $v_{\text{in}} < v_{\text{cr}}$ where, even though these velocities are below the critical speed, the kinks escape to infinities after two, three, four etc. collisions. Our analysis of two-bounce escape windows shows that their positions and structure are well described by the phenomenological resonance condition, with the corresponding resonance frequency being close to the frequency of the kink's vibrational mode. This confirms the resonant energy exchange between the kink's translational mode and its vibrational mode (or, more precisely, a localised excitation of the kink-kink system that is close to the vibrational mode of a solitary kink) as the driving mechanism that leads to the occurrence of escape

windows in kink-kink collisions in that sector of the φ^8 model.

Finally, we would like to reflect on several issues that have been left out of the scope of this work but represent interest for future research.

1. Some of the kinks of the φ^8 model, corresponding to particular choices of the model parameters, can have power-law, rather than exponential, asymptotic at the spatial infinity [35]. Studying these kinks along the lines of our work would be a natural extension of this work.
2. Resonant energy exchange in kink-kink collisions can also occur when the corresponding solitary kinks do not have vibrational excitations. For instance, two colliding kinks can have a collective vibrational mode, even though each of the two solitary waves does not. This has been shown to happen in the φ^6 and the double-sine-Gordon models [36, 37]. This situation, apparently, can take place in some variants of the φ^8 model.
3. We think (in agreement with the authors of ref. [35]) that the collective coordinate method could be productively applied to studying kink-kink interaction in this model. It is worth noting that kinks with power-law asymptotic can apparently result in power-law asymptotic of the collective potential, which is a new feature that does not occur in other field models, such as, e.g., φ^4 and φ^6 .

Acknowledgements

The authors are very grateful to Prof. A. E. Kudryavtsev for his interest to their work and for enlightening discussions. This work was supported in part by the Russian Federation Government under grant No. NSh-3830.2014.2. V. A. Gani acknowledges support of the Ministry of Education and Science of the Russian Federation, Project No. 3.472.2014/K. M. A. Lizunova and V. Lensky thank the ITEP support grant for junior researchers. M. A. Lizunova also gratefully acknowledges financial support from the Dynasty Foundation.

-
- [1] A. Vilenkin and E. P. S. Shellard, *Cosmic Strings and Other Topological Defects* (Cambridge University Press, Cambridge, 2000).
 - [2] N. Manton, P. Sutcliffe, *Topological Solitons* (Cambridge University Press, Cambridge, 2004).

- [3] T. I. Belova and A. E. Kudryavtsev, Usp. Fiz. Nauk **167**, 377 (1997) [Phys.-Usp. **40**, 359 (1997)].
- [4] G. L. Alfimov, A. S. Malishevskii, and E. V. Medvedeva, Physica D **282**, 16 (2014).
- [5] P. Ahlqvist, K. Eckerle, and B. Greene, JHEP **04**, 059 (2015); arXiv: 1411.4631 [hep-th].
- [6] E. Greenwood, E. Halstead, R. Poltis, and D. Stojkovic, Phys. Rev. D **79**, 103003 (2009).
- [7] R. Poltis, arXiv: 1201.6362 [hep-ph].
- [8] E. Braaten and L. Carson, Phys. Rev. D **38**, 3525 (1988).
- [9] D. Foster and N. S. Manton, arXiv: 1505.06843 [nucl-th].
- [10] M. B. Hindmarsh and T. W. B. Kibble, Rept. Prog. Phys. **58**, 477 (1995).
- [11] E. J. Copeland and T. W. B. Kibble, Proc. Roy. Soc. Lond. A **466**, 623 (2010); arXiv: 0911.1345 [hep-th].
- [12] M. Quandt, N. Graham, and H. Weigel, Phys. Rev. D **87**, 085013 (2013); arXiv: 1303.0178 [hep-th].
- [13] O. Schroeder, N. Graham, M. Quandt, and H. Weigel, J. Phys. A **41**, 164049 (2008); arXiv: 0710.4386 [hep-th].
- [14] H. Weigel, M. Quandt, and N. Graham, Int. J. Mod. Phys. A **27**, 1260016 (2012); arXiv: 1111.4863 [hep-th].
- [15] R. V. Palvelev, Teor. Mat. Fiz. **156**, 77 (2008) [Theor. Math. Phys. **156**, 1028 (2008)].
- [16] J. Dziarmaga, Phys. Rev. D **51**, 7052 (1995); arXiv: hep-th/9412180.
- [17] E. Myers, C. Rebbi, and R. Strilka, Phys. Rev. D **45**, 1355 (1992).
- [18] P. M. Sutcliffe, Int. J. Mod. Phys. A **12**, 4663 (1997).
- [19] R. S. Ward, Phys. Lett. A **208**, 203 (1995).
- [20] L. P. Pitaevskii, ZhETF **146**, 1252 (2014) [JETP **119**, 1097 (2014)].
- [21] A. Yu. Loginov, ZhETF **145**, 250 (2014) [JETP **118**, 217 (2014)].
- [22] A. Yu. Loginov, Pis'ma v ZhETF **100**, 385 (2014) [JETP Lett. **100**, 346 (2014)].
- [23] S. W. Goatham, L. E. Mannering, R. Hann, and S. Krusch, Acta Physica Polonica B **42**, 2087 (2011); arXiv: 1007.2641 [hep-th].
- [24] S. P. Popov, Zh. Vychisl. Mat. Mat. Fiz. **53**, 2072 (2013) [Comput. Math. Math. Phys. **53**, 1891 (2013)].
- [25] S. P. Popov, Zh. Vychisl. Mat. Mat. Fiz. **54**, 1954 (2014) [Comput. Math. Math. Phys. **54**, 1876 (2014)].

- [26] A. M. Gumerov, E. G. Ekomasov, F. K. Zakir'yanov, R. V. Kudryavtsev, Zh. Vychisl. Mat. Mat. Fiz. **54**, 481 (2014) [Comput. Math. Math. Phys. **54**, 491 (2014)].
- [27] D. Saadatmand, S. V. Dmitriev, D. I. Borisov, and P. G. Kevrekidis, Phys. Rev. E **90**, 052902 (2014); arXiv: 1408.2358 [nlin.PS].
- [28] D. Saadatmand, S. V. Dmitriev, D. I. Borisov, P. G. Kevrekidis, M. A. Fatykhov, and K. Javidan, Pis'ma v ZhETF **101**, 550 (2015) [JETP Lett. **101**, 497 (2015)].
- [29] D. Saadatmand, S. V. Dmitriev, D. I. Borisov, P. G. Kevrekidis, M. A. Fatykhov, and K. Javidan, Commun. Nonlinear Sci. Numer. Simulat. **29**, 267 (2015); arXiv: 1411.5857 [nlin.PS].
- [30] Z. Fei, Yu. S. Kivshar, and L. Vazquez, Phys. Rev. A **45**, 6019 (1992).
- [31] T. S. Mendonça and H. P. de Oliveira, arXiv: 1502.03870 [hep-th]; arXiv: 1504.07315 [hep-th].
- [32] M. A. Lohe, Phys. Rev. D **20**, 3120 (1979).
- [33] S. V. Pavlov, M. L. Akimov, Crystall. Rep. **44**, 297 (1999).
- [34] (a) E. B. Bogomolny, Yad. Fiz. **24**, 861 (1976); Sov. J. Nucl. Phys. **24**, 449 (1976); (b) M. K. Prasad and C. M. Sommerfield, Phys. Rev. Lett. **35**, 760 (1975).
- [35] A. Khare, I. C. Christov, and A. Saxena, Phys. Rev. E **90**, 023208 (2014); arXiv: 1402.6766 [math-ph].
- [36] P. Dorey, K. Mersh, T. Romanczukiewicz, and Y. Shnir, Phys. Rev. Lett. **107**, 091602 (2011); arXiv: 1101.5951 [hep-th].
- [37] V. A. Gani and A. E. Kudryavtsev, Phys. Rev. E **60**, 3305 (1999); arXiv: cond-mat/9809015.
- [38] D. Campbell, M. Peyrard, and P. Sodano, Physica D **19**, 165 (1986).
- [39] M. Peyrard and D. Campbell, Physica D **9**, 33 (1983).
- [40] V. A. Gani, A. E. Kudryavtsev, and M. A. Lizunova, Phys. Rev. D **89**, 125009 (2014); arXiv: 1402.5903 [hep-th].